

# Supporting Information

## A High-Performance Li-Metal Free Sulfur Battery Employing Lithiated Anatase TiO<sub>2</sub> Anode and Free Standing Li<sub>2</sub>S-Carbon Aerogel Cathode

*Ravindra Kumar Bhardwaj<sup>1</sup>, Homen Lahan<sup>1</sup>, Venkataraman Sekkar<sup>2#</sup>, Bibin John<sup>2</sup> and Aninda J. Bhattacharyya<sup>1\*</sup>*

*<sup>1</sup>Solid State and Structural Chemistry Unit, Indian Institute of Science, Bengaluru-560012, India*

*<sup>2</sup>ISRO-VSSC, Thiruvananthapuram, 695022, India*

*\*Email: anindajb@iisc.ac.in*

**Number of pages: 15**

**Number of figures: 17**

**Number of tables: 02**

---

<sup>#</sup> Present Address: School of Environmental Studies, Cochin University of Science and Technology (CUSAT), Kochi - 682 022; Kerala, India

## **Table of content**

Figure S1	X-ray diffraction pattern of TiO <sub>2</sub> nanoparticles	Page 3
Figure S2	Schematic of cell used for operando Raman measurements	Page 4
Figure S3	Bright-field TEM image of Li <sub>2</sub> S nanostructure	Page 4
Figure S4	Bright-field TEM image of pelletized Li <sub>2</sub> S/CA cathode	Page 5
Figure S5	Powder-XRD pattern of Li <sub>2</sub> S powder (blue), CA (green) and Li <sub>2</sub> S/CA pellet red	Page 5
Figure S6	N <sub>2</sub> adsorption/desorption isotherms of CA	Page 6
Figure S7	SEM image and elemental mapping of Li <sub>2</sub> S	Page 6
Figure S8	SEM image and elemental mapping of CA	Page 7
Figure S9	SEM image and elemental mapping of Li <sub>2</sub> S/CA composite cathode	Page 7
Figure S10	SEM image and elemental mapping of Li <sub>2</sub> S/CA cathode after activation cycle	Page 7
Figure S11	Schematic of the symmetric cell employed for measuring the tortuosity of the Li <sub>2</sub> S/CA pellet	Page 8
Figure S12	Nyquist plot and equivalent circuit for the Li <sub>2</sub> S/CA pellet	Page 8
Figure S13	Electrochemical Impedance spectroscopy (EIS, Nyquist plot) of the Li/S cell with Li <sub>2</sub> S/CA cathode	Page 9
Figure S14	Galvanostatic charge/discharge profile of Li <sub>2</sub> S/Gr full cell	Page 10
Figure S15	Cyclic voltammograms of Li <sub>2</sub> S/Gr full cell	Page 10
Figure S16	Electrochemical Impedance spectroscopy (EIS, Nyquist plot) of the Li  TiO <sub>2</sub> cell and Li  Gr cell	Page 11
Figure S17	Galvanostatic charge/discharge profile at various current rate	Page 11
Table S1	Comparison of the energy density of the present work with other previously reported Li <sub>2</sub> S based full cells	Page 12
Table S2	A comparison of the energy density of the Li <sub>2</sub> S/CA  TiO <sub>2</sub> cell with the commercial LIBs comprising intercalation compounds cathode and graphite anode	Page 14

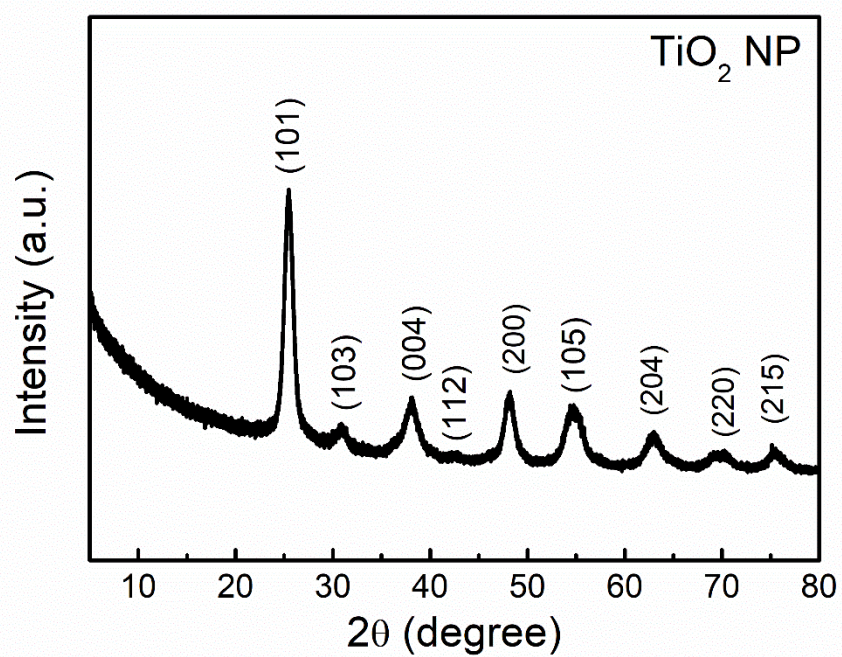


**Figure S1.** X-ray diffraction pattern of TiO<sub>2</sub> nanoparticles

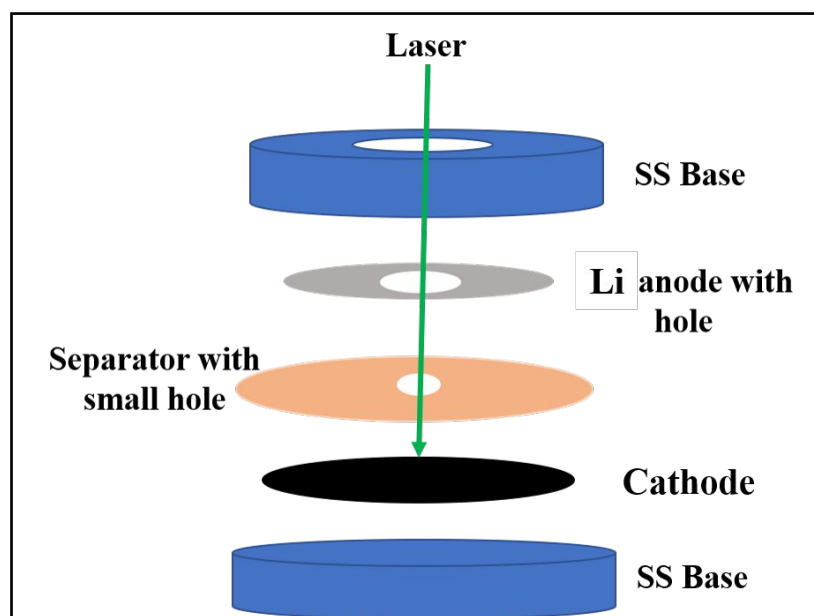


**Figure S2.** Schematic of cell used for operando Raman measurements

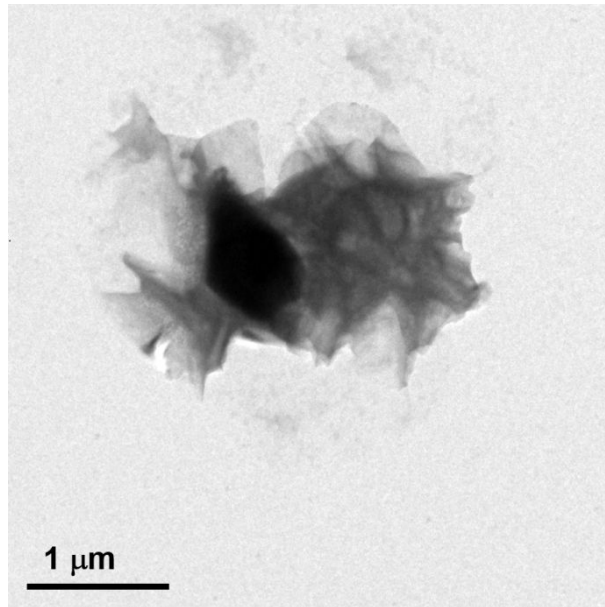


**Figure S3.** Bright-field TEM image of  $\text{Li}_2\text{S}$  nanostructure

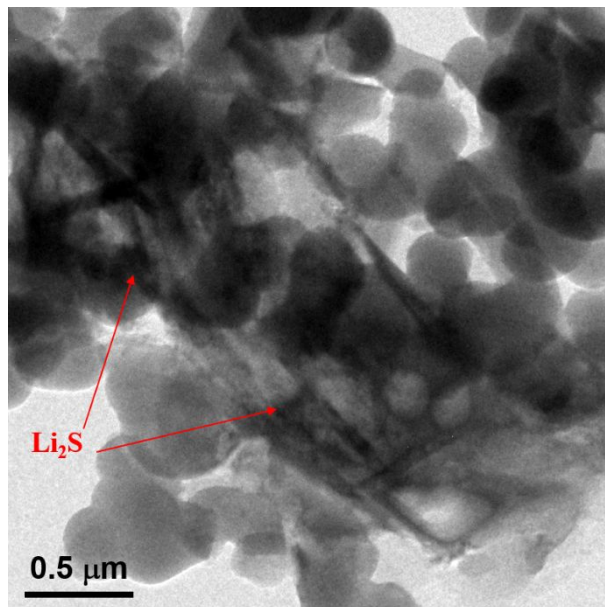


**Figure S4.** Bright-field TEM image of pelletized  $\text{Li}_2\text{S}/\text{CA}$  cathode.

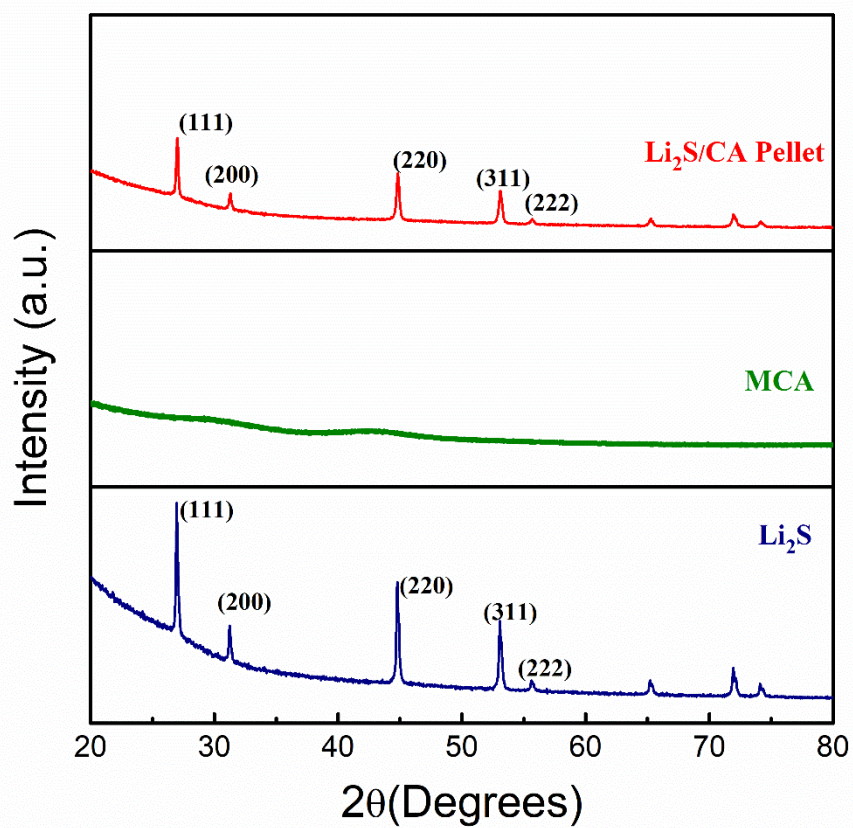


**Figure S5.** Powder-XRD pattern of  $\text{Li}_2\text{S}$  powder (blue), CA (green) and  $\text{Li}_2\text{S}/\text{CA}$  pellet red.

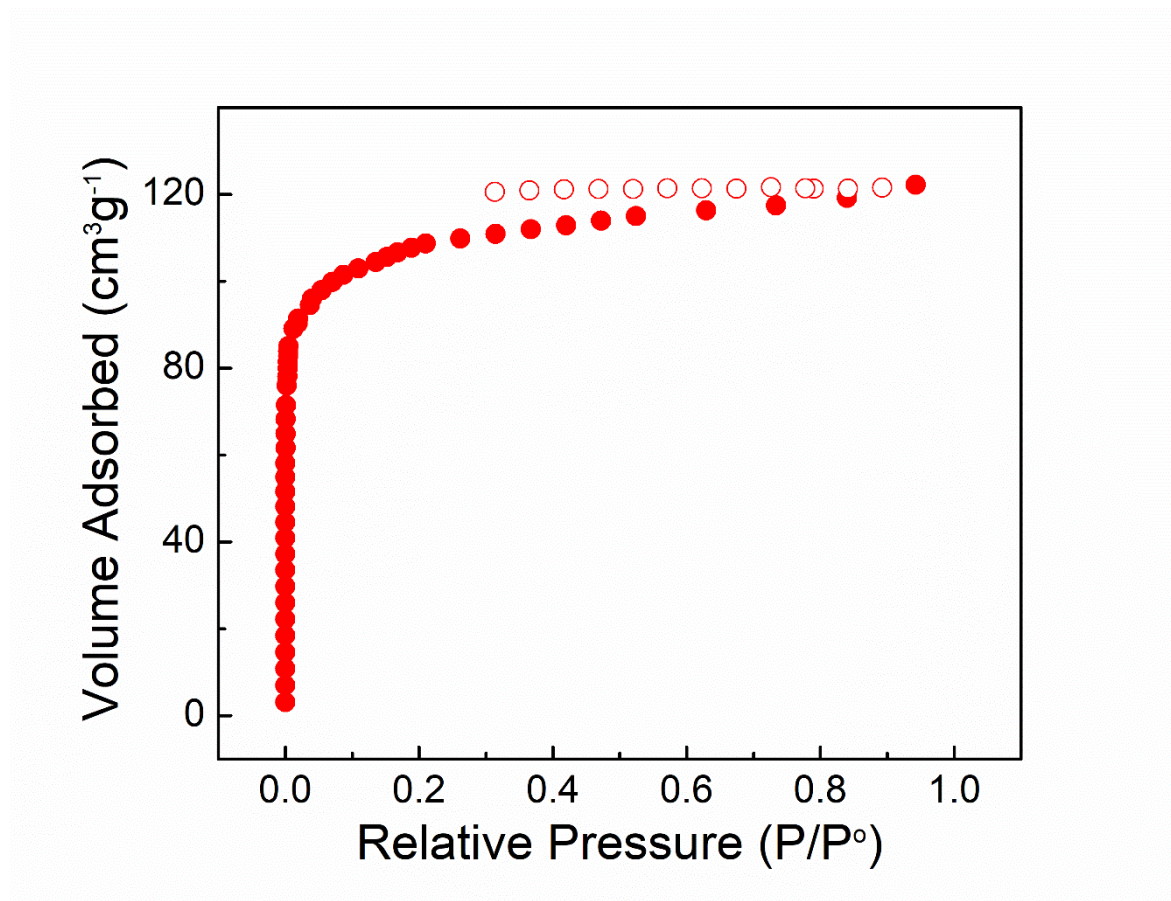


**Figure S6.** N<sub>2</sub> adsorption/desorption isotherms of CA

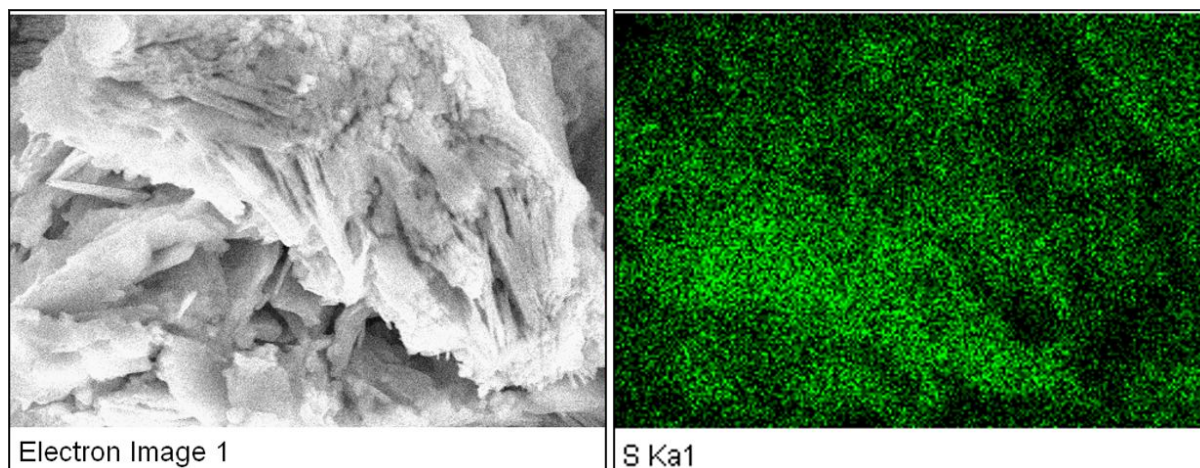


**Figure S7.** SEM image and elemental mapping of Li<sub>2</sub>S

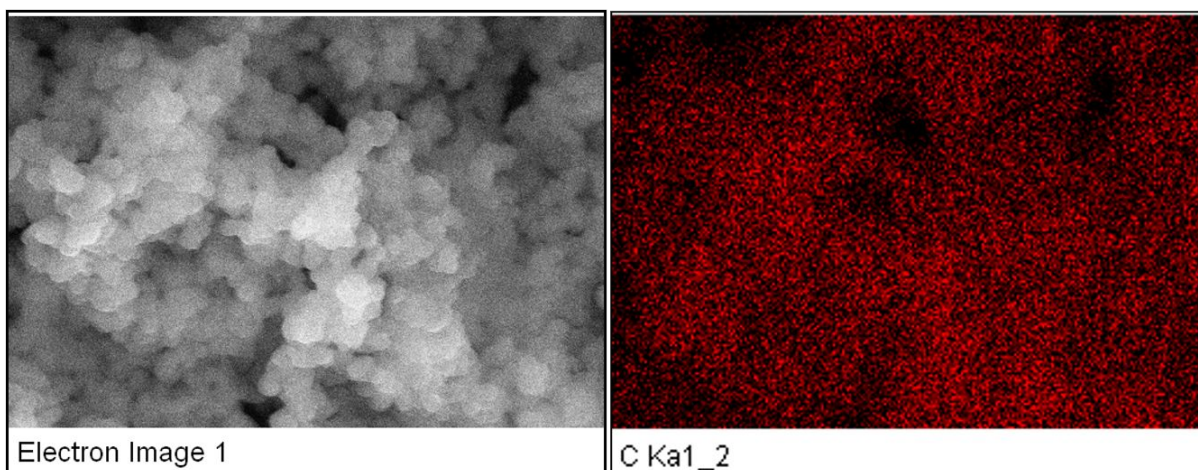


**Figure S8.** SEM image and elemental mapping of CA

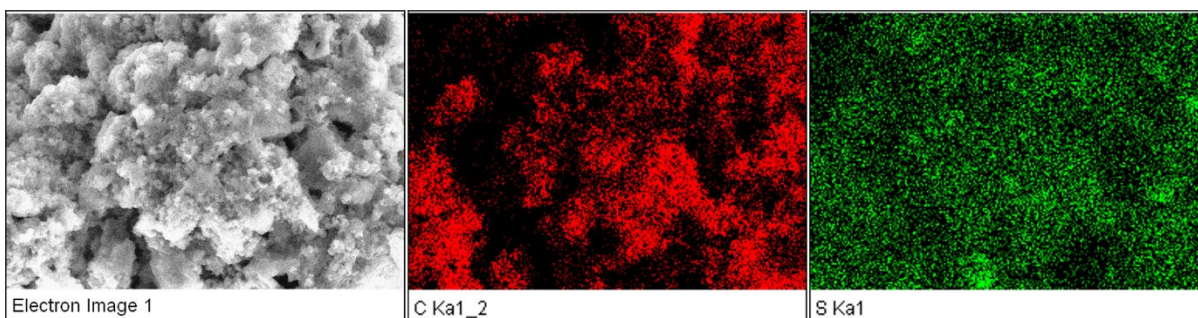


**Figure S9.** SEM image and elemental mapping of  $\text{Li}_2\text{S}/\text{CA}$  composite cathode

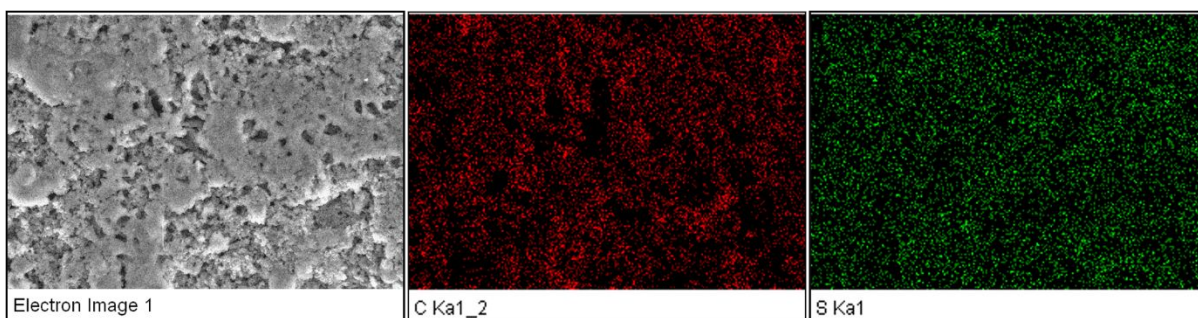


**Figure S10.** SEM image and elemental mapping of  $\text{Li}_2\text{S}/\text{CA}$  cathode after activation cycle.

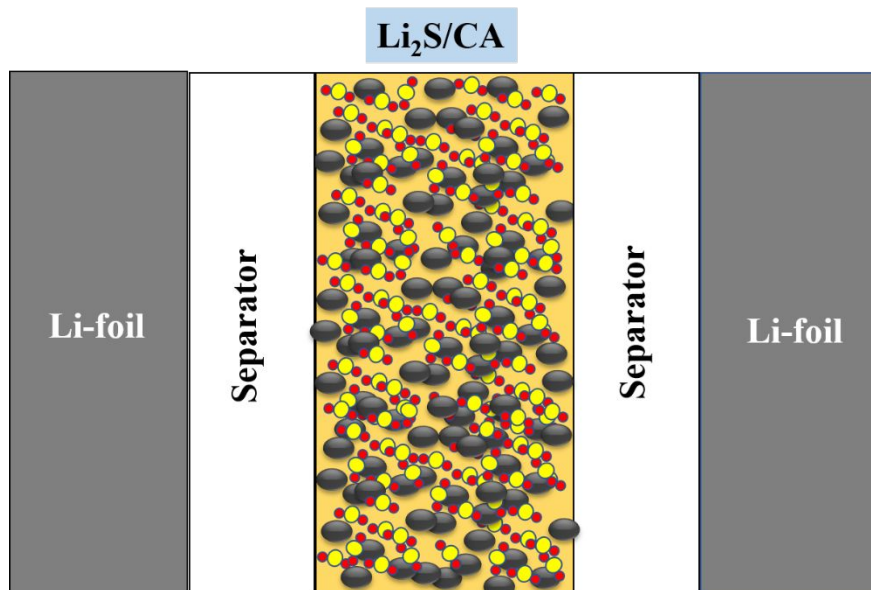


**Figure S11.** Schematic of the symmetric cell employed for measuring the tortuosity of the Li<sub>2</sub>S/CA pellet.

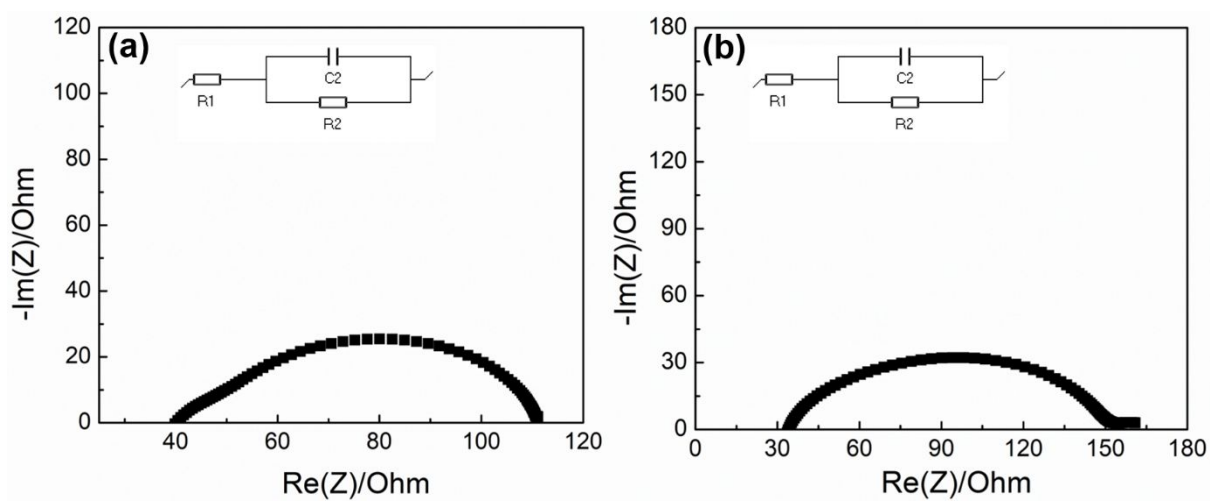


**Figure S12.** Nyquist plot and equivalent circuit for the Li<sub>2</sub>S/CA pellet obtained (a) Without separator, (b) With separator.



The Li<sub>2</sub>S/CA pellet is placed between separators placed between lithium foil electrodes. The tortuosity was obtained using the following expression:

$$\sigma_p = \sigma \phi \tau^{-1} \dots \dots \dots S1$$

where,

$\sigma_p$ : effective conductivity (with separator as figure S10) =  $7.14 \times 10^{-5}$  S/cm

$\sigma$ : intrinsic conductivity (without separators) =  $1.2 \times 10^{-4}$  S/cm

$\phi$ : Volume fraction of pores = 0.60

$\tau$ : Tortuosity of the materials as per equation S1 = 1.06

$\sigma_p$  and  $\sigma$  are ionic conductivity in the presence and absence of separator. Volume fraction of pores were obtained by estimating the density from calculated sample volume and weight.

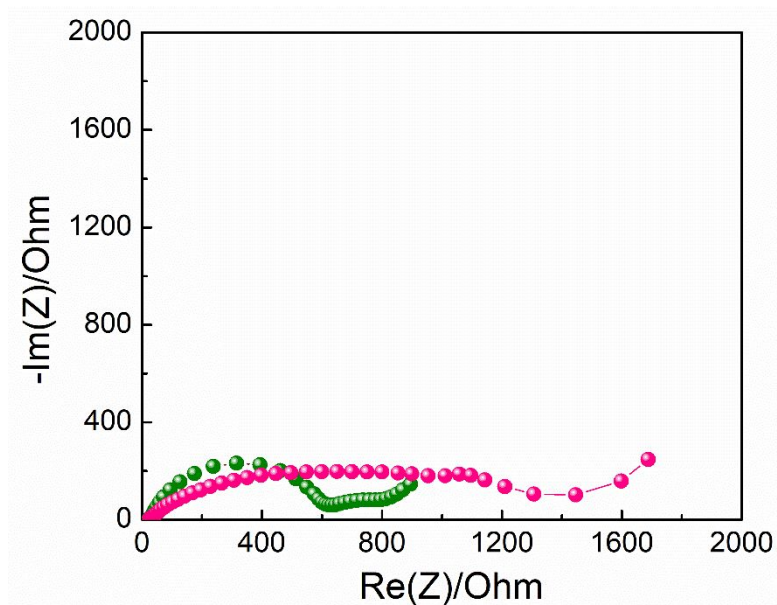


**Figure S13.** Electrochemical Impedance spectroscopy (EIS, Nyquist plot) of the Li/S cell with Li<sub>2</sub>S/CA cathode, at OCV (green), after activation (pink).

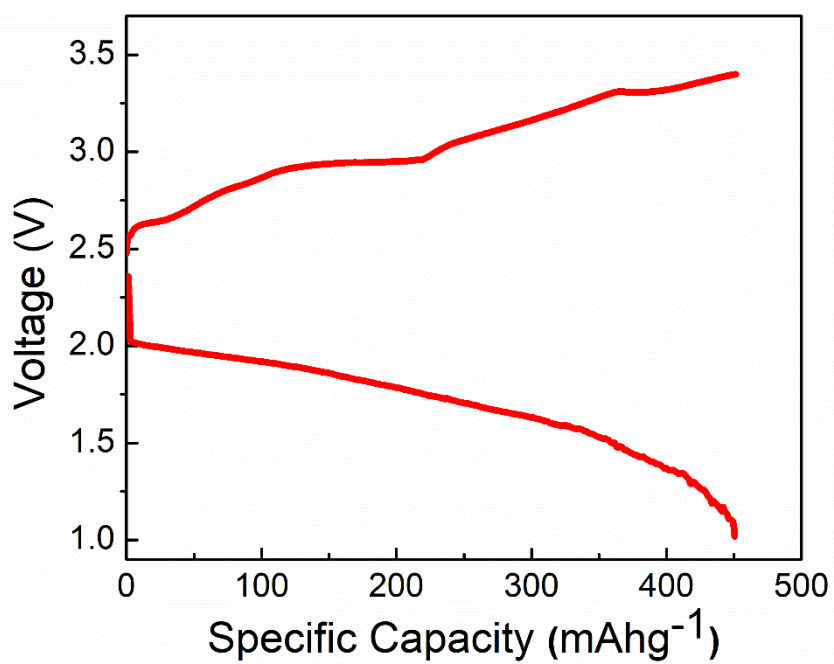


**Figure S14.** Galvanostatic charge/discharge profile of Li<sub>2</sub>S/Gr full cell

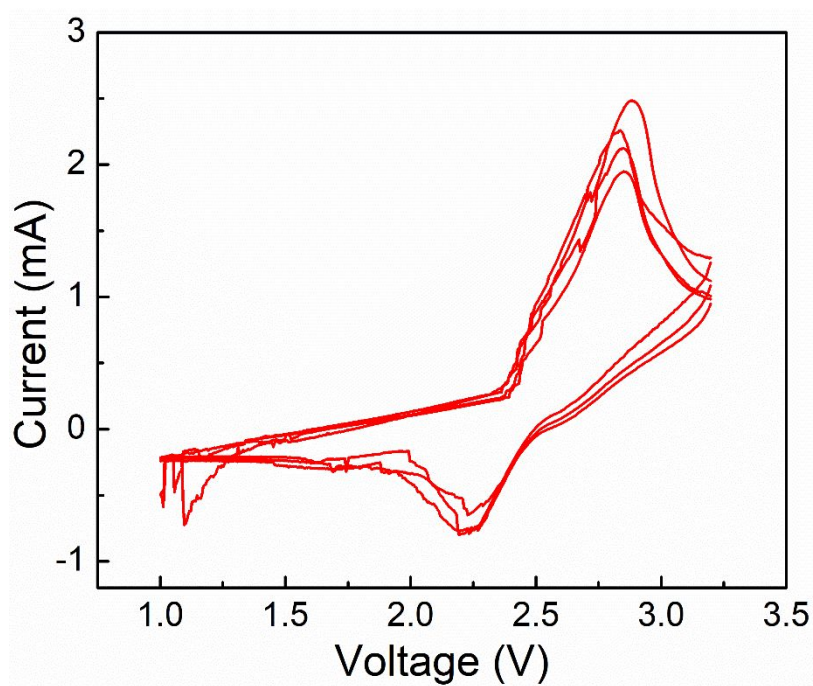


**Figure S15.** Cyclic voltammograms of Li<sub>2</sub>S/Gr full cell.

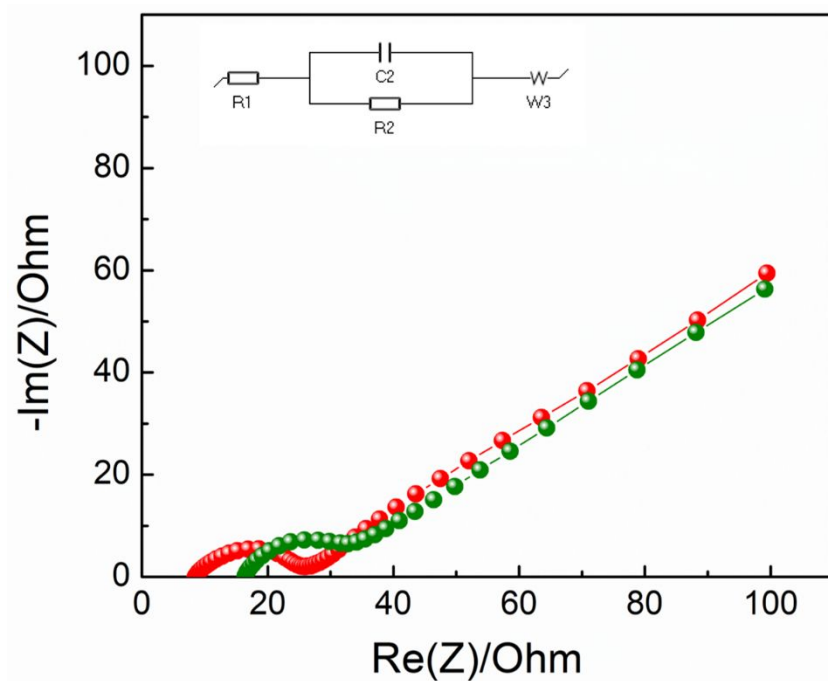


**Figure S16.** Electrochemical Impedance spectroscopy (EIS, Nyquist plot) of the Li||TiO<sub>2</sub> cell (red) and Li||Gr cell (green). Inset shows the equivalent circuit for fitting the data.

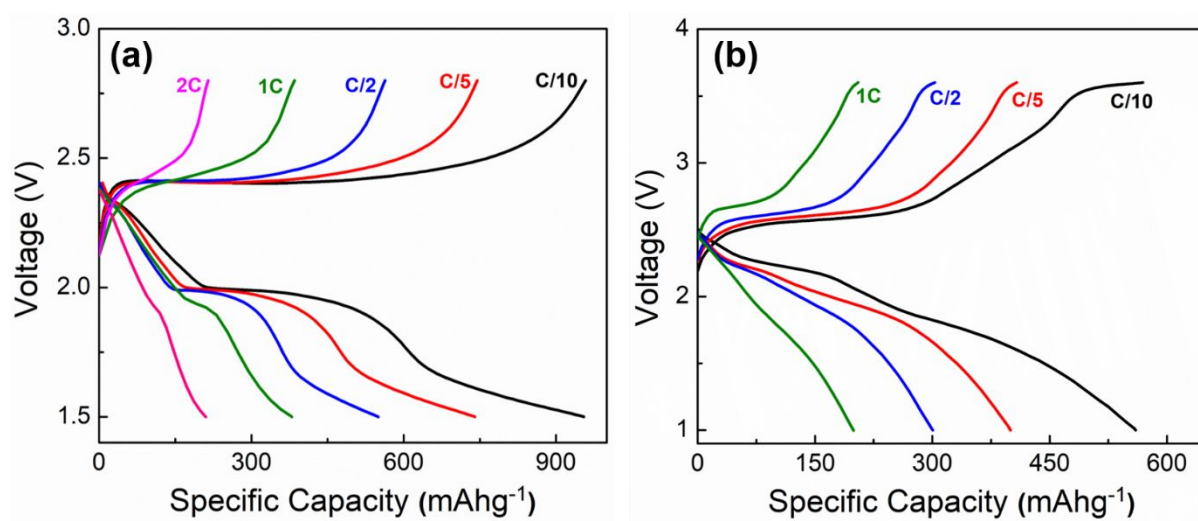


**Figure S17.** Rate capability of the Li-S cell with (a) Li<sub>2</sub>S/CA cathode and lithium anode, (b) Li<sub>2</sub>S/CA cathode and TiO<sub>2</sub> anode

**Table S1.** A comparison of the energy density of the present work with other previously reported Li<sub>2</sub>S based full cells.

Cathode	Anode	Capacity @ first discharge	Number of cycles	Energy Density (Wh/kg)	Reference
Li <sub>2</sub> S mesoporous carbon composite cathode	Silicon nanowire anode	423 mAh g <sup>-1</sup>	20	720	1
Li <sub>2</sub> S-MCMB composite	Si-O-C anode	228 mAh g <sup>-1</sup>	50	390	2
Li <sub>2</sub> S/C composite Cathode	Graphite anode	750 mAh g <sup>-1</sup>	300	1300	3
Nano compacted Li <sub>2</sub> S/Graphene composite	Graphene	800 mAh g <sup>-1</sup>	100	1400	4
Li <sub>2</sub> S/Carbon aerogel pellet cathode	Anatase TiO <sub>2</sub> anode	566 mAh g <sup>-1</sup>	200	1300	Current work

Cell parameters of the Li<sub>2</sub>S/TiO<sub>2</sub> cell using TiO<sub>2</sub> anode and Li<sub>2</sub>S/CA cathode

Materials	Weight (mg)
Li <sub>2</sub> S	7.8
Carbon aerogel (CA)	3.4

TiO <sub>2</sub>	27.3
Carbon (acetylene black)	3.4
PVDF binder	3.4
Al-Current collector	5.0
electrolyte	87.5
Separator	13.2
<b>Total weight</b>	<b>151</b>

Cell capacity (mAh) = 4.41

Nominal cell voltage (V) = 2.3 V

Energy density of the cell based on the active mass of Li<sub>2</sub>S =  $\frac{\text{Cell capacity}}{\text{weight of Li}_2\text{S(g)}} \times \text{Cell voltage}$

..S2

$$= \frac{4.41}{7.8 \times 10^{-3}} \times 2.3$$

$$\approx 1300 \text{ Wh/Kg}$$

Energy density of the cell based on the total weight of the cell =  $\frac{\text{Cell capacity}}{\text{total weight (g)}} \times \text{Cell voltage}$

$$= \frac{4.41}{151 \times 10^{-3}} \times 2.3$$

$$\approx 30 \text{ Wh/Kg}$$

**Table S2.** A comparison of the energy density of the Li<sub>2</sub>S/CA||TiO<sub>2</sub> cell with the commercial LIBs comprising intercalation compounds cathode and graphite anode.

Cell Chemistry	Anode	Cathode	Nominal Voltage	Energy Density (Wh/kg)
Lithium cobalt oxide	Graphite	LiCoO <sub>2</sub>	3.7	195
Lithium iron phosphate	Graphite	LiFePO <sub>4</sub>	3.2	160
<u>Lithium nickel cobalt aluminium oxides</u>	Graphite	NCA	3.6	220
<u>Lithium nickel manganese cobalt oxide</u>	Graphite	NMC	3.6	205
Li <sub>2</sub> S/Carbon aerogel pellet cathode	Anatase TiO <sub>2</sub> anode	Li <sub>2</sub> S/CA pellet	2.3	1300 (Current work)

## REFERENCES

- (1) Hwang, J.; Shin, S.; Yoon, C. S.; Sun, Y.; Shin, S.; Yoon, C. S.; Sun, Y. Nano-Compacted Li<sub>2</sub>S/Graphene Composite Cathode for High-Energy Lithium–Sulfur Batteries. *ACS Energy Lett.* **2019**, *4*, 2787–2795, DOI 10.1021/acseenergylett.9b01919.
- (2) Yang, Y.; McDowell, M. T.; Jackson, A.; Cha, J. J.; Hong, S. S.; Cui, Y. New Nanostructured Li<sub>2</sub>S/Silicon Rechargeable Battery with High Specific Energy. *Nano Lett.* **2010**, *10* (4), 1486–1491, DOI 10.1021/nl100504q.
- (3) Agostini, M.; Hassoun, J.; Liu, J.; Jeong, M.; Nara, H.; Momma, T.; Osaka, T.; Sun, Y. K.; Scrosati, B. A Lithium-Ion Sulfur Battery Based on a Carbon-Coated Lithium-Sulfide Cathode and an Electrodeposited Silicon-Based Anode. *ACS Appl. Mater. Interfaces* **2014**, *6* (14), 10924–10928, DOI 10.1021/am4057166.

- (4) Seita, T.; Matsumae, Y.; Liu, J.; Tatara, R.; Ueno, K.; Dokko, K.; Watanabe, M.  
Graphite-Lithium Sulfide Battery with a Single-Phase Sparingly Solvating Electrolyte.  
*ACS Energy Lett.* **2020**, *5* (1), 1–7, DOI 10.1021/acseenergylett.9b02347.